

## Research Article

# An Energy Solution for Predicting Buried Pipeline Response Induced by Tunneling Based on a Uniform Ground Movement Model

Xin Shi <sup>1,2</sup>, Chuanxin Rong <sup>1,2</sup>, Hua Cheng <sup>2</sup>, Linzhao Cui <sup>3</sup>, and Jie Kong <sup>2</sup>

<sup>1</sup>State Key Laboratory of Mining Response and Disaster Prevention and Control in Deep Coal Mine, Anhui University of Science and Technology, Huainan 232001, China

<sup>2</sup>School of Civil Engineering and Architecture, Anhui University of Science and Technology, Huainan 232001, China

<sup>3</sup>Anhui Water Resources Development Co.Ltd, Bengbu 233000, China

Correspondence should be addressed to Chuanxin Rong; rongcx@ustc.edu

Received 6 December 2019; Accepted 11 February 2020; Published 19 March 2020

Academic Editor: Piero Colajanni

Copyright © 2020 Xin Shi et al. This is an open access article distributed under the Creative Commons Attribution License, which permits unrestricted use, distribution, and reproduction in any medium, provided the original work is properly cited.

The construction of shield tunnels inevitably causes displacement of the surrounding soil and additional stress and deformation of the buried pipeline. An energy solution for predicting the deformation of buried pipelines caused by tunneling is proposed in this study. First, based on the uniform ground movement model, the interval of the free displacement field of soil around the pipeline induced by tunneling is calculated. Then, we use the Pasternak model to establish the total potential energy equation of the tunnel-soil-pipeline interaction. The final settlement interval of the pipeline is obtained by solving the numerical calculation program with MATLAB. The calculation results of the energy solution are compared with the results of the centrifugal test and the reported theoretical solutions of Winkler and Pasternak, and then the applicability of the solution for predicting the pipeline response under different geotechnical conditions is verified. Combined with an engineering case, the energy method calculation results, numerical simulation results, and measured results are compared to obtain the most unfavorable position of the pipeline caused by tunneling. At the end of this study, the application steps of the proposed method in actual construction are summarized. These steps are used to predict pipeline response in order to take protective measures.

## 1. Introduction

With the acceleration of urbanization, subway construction is becoming more and more popular. During the construction process, disturbances to the surrounding soil are inevitable. When the amount of deformation of the soil is too large, construction can easily cause damage to adjacent underground pipelines and even accidents, such as breakage or bursting. Therefore, it is necessary to correctly analyze the deformation of pipelines during the tunnel excavation.

At present, the methods for studying the effects of tunnel excavation on pipelines include analytical methods, centrifugal tests, and numerical simulations. In terms of analytic methods, Huang et al. [1] proposed a Winkler solution based on an improved Winkler modulus to

analyze the jointed pipeline response caused by tunnel excavation. The rationality of this method was verified by the reported elastic continuous solution, field measurement data, and centrifugal test data. Yu et al. [2] gave the expression of the Winkler subgrade modulus of a pipeline buried at an arbitrary depth and arbitrary curved shape free soil displacement. Based on the superposition principle and Fourier integral, the subgrade modulus of an infinite beam resting on an elastic half space and buried infinitely are obtained, respectively, and its effectiveness is verified. Ni and Mangalathu et al. [3] discussed the probability risk of gray iron pipes caused by tunneling. Previous studies have found that existing pipelines with smaller pipe diameters and larger pipe wall thicknesses buried at shallower depths in loosely compacted soils with

smaller soil friction angles are less prone to failure due to tunneling-induced ground settlement. Liu et al. [4] used the energy variation analysis method to calculate the vertical displacement of the pipeline caused by tunnel excavation based on the Winkler model.

Saiyar et al. [5] used a centrifugal test of four glass pipe models to measure the kinematics associated with a cast-iron pipe fracture and the relative rotation of the pipe on both sides caused by a normal ground fracture. Ma et al. [6] used three-dimensional centrifugal model tests and the advanced hypoplasticity constitutive model to study the effects of twin stacked tunneling with different construction sequences on existing pipelines. Vorster et al. [7] proposed a method that considers soil nonlinearity to estimate the maximum bending moment of a continuous or rigid connected pipe affected by the ground movement caused by the shield. The validity of the method as an upper bound approximation is evaluated against the centrifuge test results.

In terms of numerical simulation, some scholars have further complicated the model based on the deformation of rock and soil caused by tunnel excavation, considering the interaction between the stratum and pipeline [8–12]. Zhang et al. [10] studied the effects of pipeline parameters, foundation pit parameters, soil parameters, and underground continuous walls on pipeline stress, strain, and deformation by establishing a three-dimensional model of pipelines and foundation pits. Shi et al. [11] conducted an extensive numerical parameter study using 540 numerical runs to investigate the effects of tunnel construction on existing pipelines in clay. Wang et al. [12] studied the influence of ground movement caused by tunneling on pipelines through the finite element method and focused on the response of different soils to uplift and downward pipe-soil relative movements. Through a 900-time numerical parameter simulation test, various combinations of ground settlement profiles, pipe dimensions, material properties, pipe depth, and soil properties were studied.

Based on the uniform ground movement model, this study proposes an energy solution for calculating the pipeline response caused by tunnel excavation. Firstly, by comparing the energy solution with the results of centrifugal tests and the reported theoretical solutions of Winkler and Pasternak, the applicability of this method to predict pipeline settlement caused by tunneling is verified. In addition, for the settlement of pipelines with different geotechnical conditions, the settlement interval calculated by this method can accurately match the reported theoretical prediction curves. Afterwards, combined with an example of a circular concrete rainwater pipe culvert of Hefei Metro, China, the theoretical calculation results, numerical simulation results, and measured results were compared, and the most unfavorable position of the pipeline caused by tunneling was obtained. Eventually, the application steps of the proposed method in engineering were discussed to predict the pipeline response, in order to take protective measures.

## 2. Uniform Ground Movement Model and Energy Solution

**2.1. Calculation Model and Assumptions.** Figure 1 shows the calculation model of this study. The infinitely long pipeline is located directly above the tunnel, and the two intersect perpendicularly, where  $Z_0$  is the buried depth of the pipeline,  $h$  is the buried depth of the tunnel,  $R$  is the tunnel radius, and  $i_s$  and  $i_p$  are the distances from the tunnel centre line to the inflection point of the settlement trough of the soil and the pipeline, respectively. Only the vertical deformation of the pipeline is considered, ignoring the effect of horizontal displacement on the pipeline. To guarantee the calculation accuracy, the calculation range of the pipeline settlement in this study is  $20 i_p$  (the half width is  $10 i_p$ ).

The current problem is a hypothetical situation based on the behavior of linear elastic soils with small displacements of the soil using the following assumptions:

- (1) The influence of the presence of the pipeline on the tunnel is negligible.
- (2) The deformation of the soil at the buried depth of the pipeline has no effect on the tunnel.
- (3) The soil and the pipeline are always in contact.

**2.2. Uniform Ground Movement Model.** Wei [13] found that there are two extreme states of ground movement. When the mechanical properties of soil are poor, after passing the shield tail, the surrounding soil will quickly close the gap between the shield shell and the lining, and the soil will be adsorbed on the outer wall of the lining without falling down. The soil has a tendency to move toward the center point of the tunnel, which is called the focus. At this moment in the process, the focus is close to the center point of the tunnel, and, in the limit case, the focus is at the center point of the tunnel, as shown in Figure 2(a).

When the soil quality is good, after the shield tail passes, the soil does not immediately close the gap, and the soil particles fall down due to their own weight. Palmer and Belshaw [14] analyzed the measured data and pointed out that the soil around the tunnel has a tendency to move toward the bottom of the tunnel, rather than toward the center of the tunnel. There is almost no deformation of the soil below the bottom of the tunnel. When the soil has a tendency to move toward the bottom of the tunnel, the focus is close to the bottom, and, in the extreme case, the focus is at the bottom of the tunnel, as shown in Figure 2(c). When the soil condition is between the abovementioned two, the focus is between the center point and the bottom position of the tunnel, as shown in Figure 2(b).

Wei Gang et al. established a uniform movement model of soil by defining the distance from the focus to the center point of the tunnel as  $d$ , and its range is  $[0, R]$ . When  $d = 0$ , the model is equal to the Park model [15]; when  $d = g/2$ ,  $g$  is the equivalent soil loss parameter (m), and the model is

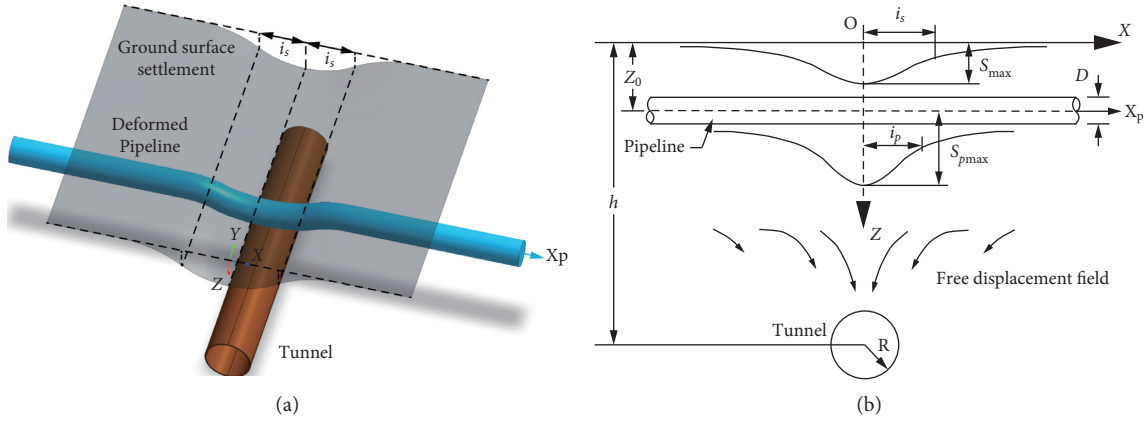
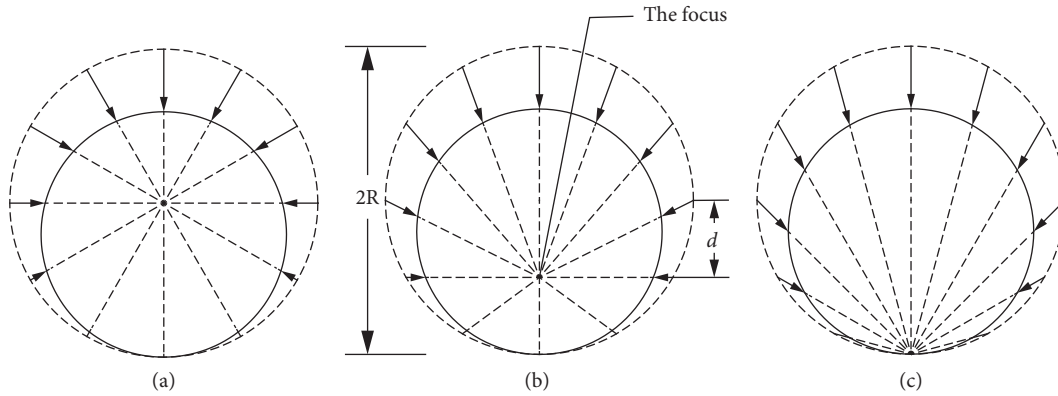


FIGURE 1: Calculation model: (a) three-dimensional view; (b) deformation along the pipeline direction.


 FIGURE 2: Uniform ground movement model: (a) limit state 1: soil is the poorest,  $d = 0$ ; (b) intermediate state:  $0 < d < R$ ; and (c) limit state 2: best soil quality,  $d = R$ .

equal to the Loganathan model [16]. Based on this model, the peak value  $S_{\max}$  of the settlement trough considering  $d$  is obtained through the closed form solutions proposed by Sagaseta. The detailed solution process can be found in the literature [17]. The expression is

$$S_{\max} = \frac{4R(h+d)}{R+d} - 4 \sqrt{R^2 \left( \frac{h+d}{R+d} \right)^2 - \frac{V_{\text{loss}}}{\pi}}, \quad (1)$$

where  $R$  is the outer radius of the tunnel (m) and  $d$  is the distance from the focus to the center point of the tunnel (m), ranging from 0 to  $R$ . Thus, the better the soil quality, the larger the value;  $h$  is the distance from the tunnel centerline to the ground (m);  $V_{\text{loss}}$  is the amount of soil loss per unit length of the tunnel ( $\text{m}^3/\text{m}$ ). According to the research of Lee et al. [18],  $V_{\text{loss}}$  is defined as

$$V_{\text{loss}} = \pi \left( \frac{Dg}{2} - \frac{g^2}{4} \right), \quad (2)$$

where  $g = G_p' + U_{3D} + \omega$ ;  $G_p' = \alpha G_p$  is the gap between the shield shell and the lining, which should be multiplied by a reduction factor  $\alpha$  to take into account the grouting fill;  $U_{3D}$  is the three-dimensional elastoplastic deformation of the soil

at the front of the shield machine, and its value is 0 for the earth pressure balance shield;  $\omega$  is the radial deformation of the end face considering the quality of the construction process (Lee et al. pointed out that  $\omega = 0.6G_p'$ ).

When  $d = 0$ , the lower bound solution is obtained as

$$S_{\max-L} = 4h - 4 \sqrt{h^2 - \frac{V_{\text{loss}}}{\pi}}. \quad (3)$$

When  $d = R$ , the upper bound solution is obtained as

$$S_{\max-U} = 2h + 2R - 2 \sqrt{(h+R)^2 - \frac{4V_{\text{loss}}}{\pi}}. \quad (4)$$

According to the Peck formula, the upper and lower solutions of the width coefficient of the settlement trough are obtained by combining equations (3) and (4):

$$i_L = \frac{V_{\text{loss}}}{S_{\max-U} \sqrt{2\pi}}, \quad (5)$$

$$i_U = \frac{V_{\text{loss}}}{S_{\max-L} \sqrt{2\pi}}.$$

Finally, the upper and lower solutions of the free displacement field of soil,  $u_{zu}$  and  $u_{zl}$ , caused by tunnel excavation, are obtained as

$$\begin{aligned} u_{zu} &= S_{\max-U} \exp\left(-\frac{x^2}{2l_U^2}\right), \\ u_{zl} &= S_{\max-L} \exp\left(-\frac{x^2}{2l_L^2}\right). \end{aligned} \quad (6)$$

From the previous analysis, the models in this study are the Park model and the Loganathan model (when  $d=0$  and  $d=g/2$ , respectively), so the free displacement field of the soil calculated by using the Park model and the Loganathan model for the same calculation parameters should be close to the lower bound solution of this study.

**2.3. Matrix Representation of the Vertical Displacement of a Pipeline.** The principle of minimum potential energy takes the displacement function as its basic unknown, and it is necessary to assume a suitable displacement function to represent the basic shape of the pipeline affected by tunneling. A large number of studies have described the vertical displacement shapes of pipelines with a normal distribution curve [19–25]. Liu et al. [4] assumed that the vertical displacement of the pipeline obeys a normal distribution curve, and the normal distribution curve function is expanded by a Fourier series. The vertical displacement of pipelines  $w_p(x)$  is represented by two independent finite matrices:

$$\begin{aligned} w_p(x) &= \{X_n\}\{a\}, \\ \{X_n\} &= \left\{1, \cos \frac{\pi x}{l}, \cos \frac{2\pi x}{l}, \cos \frac{3\pi x}{l}, \dots, \cos \frac{n\pi x}{l}\right\}, \\ \{a\} &= \{a_0, a_1, a_2, \dots, a_n\}^T, \end{aligned} \quad (7)$$

where  $l$  is the half-width of the pipeline settlement trough caused by tunnel excavation (i.e.,  $l = 10i_p$ );  $\{a\}$  is the non-linear parameter of the vertical displacement of the pipeline.

Assuming that the width coefficient of the pipeline settlement trough is the same as the width coefficient of the settlement trough of the soil layer where the underground pipeline is located, the empirical formula for estimating the width coefficient can be used (Mair et al. [26]):

$$i_p = \frac{0.175 + 0.325(1 - Z_0/h)}{1 - Z_0/h} (Z_0 - h). \quad (8)$$

## 2.4. Energy Equation of a Tunnel Crossing a Buried Pipeline

**2.4.1. Bending Strain Energy of Pipeline.** The pipeline can be viewed as a horizontally placed beam of diameter  $D$  and length  $2l$ . According to the theory of elastic mechanical beams, the bending strain energy of pipelines is

$$U = \int_{-L}^L \frac{E_p I_p}{2} \left( \frac{d^2 w_p}{dx^2} \right)^2 dx, \quad (9)$$

where  $U$  is the bending strain energy of the pipeline;  $E_p$  is the elastic modulus of the pipeline; and  $I_p$  is the moment of inertia of the pipeline cross section facing the central axis  $y$ .

**2.4.2. Free Soil Displacement Works on a Pipeline.** Combined with the free displacement of the soil,  $u_z$ , calculated in Section 2.2, and the final vertical displacement of the pipeline,  $w_p(x)$  (assumed in this paper), the relative displacement of the soil pipeline due to soil constraints can be obtained based on deformation coordination:

$$\Delta = u_z - w_p. \quad (10)$$

According to the Pasternak model, the earth pressure on the pipeline due to soil constraints is

$$F = -GD \frac{d^2 \Delta}{dx^2} + K\Delta, \quad (11)$$

where  $F$  is the force acting on the unit length pipeline (kN/m) and  $G$  and  $K$  are the shear modulus and the subgrade modulus of the Pasternak model, respectively. There are various methods for determining the  $G$  and  $K$  values, such as using a slab plate load test; however, the methods can be costly. In this study, the simplified elastic space method [27] is used to represent the parameters as

$$G = \frac{E}{2(1+\nu)} \left( \frac{H_s}{3} \right), \quad (12)$$

$$K = E/H_s,$$

where  $E$  is the homogeneous elastic modulus;  $\nu$  is Poisson's ratio; and  $H_s$  is the thickness of the foundation below the tunnel, which refers to the depth range affected by the additional stress at the bottom of the tunnel. According to the research of Xu [28], for strip foundations, such as tunnels and pipelines, when the ratio of the depth and width of the soil below the foundation is greater than 6, the additional stress of the base has been attenuated very small and can be ignored. Therefore, according to experience, this stress can be approximated as  $H_s = 6D$ .

From equations (12) and (13), the work conducted by the earth pressure acting on the pipeline on the pipeline can be expressed as

$$\begin{aligned} W &= \int_{-L}^L \frac{1}{2} F \Delta dx = \int_{-L}^L \frac{1}{2} \left[ -GD \frac{d^2(u_z - w_p)}{dx^2} \right. \\ &\quad \left. + KD(u_z - w_p) \right] (u_z - w_p) dx. \end{aligned} \quad (13)$$

**2.4.3. Total Potential Energy Equation.** The total potential energy  $\Pi$  is the superposition of the abovementioned pipeline bending strain energy  $U$  and the earth pressure on the pipeline work  $W$ , which can be expressed as

$$\Pi = U + W. \quad (14)$$

**2.5. Equation Solving.** Based on the principle of minimum potential energy, we solve the extreme point of the total potential energy functional  $\Pi$  of the influencing system of the tunnel construction on the pipeline. To find the extreme value of each undetermined coefficient by equation (16), we can find

$$\frac{\partial \Pi}{\partial a_i} = 0, \quad (i = 0, 1, 2, \dots, n), \quad (15)$$

where  $a_i$  is the element in the matrix  $\{a\}$ , which is the coefficient of the pipeline vertical displacement polynomial.

Solving and sorting out equation (17), the governing equations are as follows:

$$\begin{aligned} & \frac{\partial U}{\partial a_i} + \int_{-L}^L \text{KD} \frac{\partial w_p}{\partial a_i} w_p dx - \int_{-L}^L \frac{1}{2} \text{GD} \{X_n\}^T \frac{\partial^2 w_p}{\partial x^2} dx \\ & - \int_{-L}^L \frac{1}{2} \text{GD} \frac{d^2 \{X_n\}^T}{dx^2} w_p dx \\ & = \int_{-L}^L \text{KDu}_z \{X_n\}^T dx - \int_{-L}^L \frac{1}{2} \text{GD} \{X_n\}^T \frac{d^2 u_z}{dx^2} dx \\ & - \int_{-L}^L \frac{1}{2} \text{GDu}_z \frac{d^2 \{X_n\}^T}{dx^2} dx. \end{aligned} \quad (16)$$

Next, we expand and simplify equation (18), expressed in matrix form:

$$([K_p] + [K_s] + [G_s])\{a\} = \{S\}, \quad (17)$$

where  $[K_p]$  represents the pipeline stiffness;  $[K_s]$  and  $[G_s]$  represent the soil stiffness; and  $\{S\}$  represents the interaction between the free soil displacement and the underground pipeline.  $[K_p]$ ,  $[K_s]$ , and  $[G_s]$  are expressed as

$$\begin{aligned} [K_p] &= \int_{-L}^L E_p I_p \frac{\partial(\partial^2 w_p / \partial x^2)}{\partial a_i} \cdot \frac{\partial^2 \{X_n\}}{\partial x^2} dx, \\ [K_s] &= \int_{-L}^L \text{KD} \frac{\partial w_p}{\partial a_i} \{X_n\} dx, \\ [G_s] &= - \int_{-L}^L \text{GD} \{X_n\}^T \frac{d^2 \{X_n\}}{dx^2} dx. \end{aligned} \quad (18)$$

The numerical calculation program was written in MATLAB R2017, and the coefficient matrix,  $\{a\}$ , was calculated from equation (19), and then  $\{a\}$  was taken into equation (7) to obtain the final vertical displacement  $w_p(x)$  of the underground pipeline caused by tunneling.

### 3. Verification

**3.1. Comparison with the Centrifugal Test.** A series of centrifuge tests was conducted at 75 g by Vorster et al. [7] to investigate the response of jointed pipelines due to tunneling in sand. In the test, the volume loss due to tunnel excavation was simulated by gradually extracting water from the model tunnel. Vorster et al. reported settlement of the pipeline at volume losses of 0.3% and 2%, respectively. The geometric

and mechanical parameters of the pipeline and soil are shown in Table 1. According to the energy solution proposed in this study, the pipeline settlement calculated under different volume losses is compared with the centrifugal test result, as shown in Figure 3.

The centrifugal test of Vorster et al. uses sand, and the value of  $d$  trends toward 0, so the test results should be more inclined to the lower limit solution. By comparing the calculation results of the energy solution with those of the centrifugal test, it can be concluded that, under different volume losses, the shape of the settlement curve and the settlement trough width are closer to the lower limit, which is in agreement with the expected results. The maximum settlement value is higher than the lower limit value, primarily because the pipeline used in the centrifugal test has joints. Unlike the continuous pipe without joints, the existence of joints means that the deformation of the pipeline is affected by the stiffness of the joints. When the joint is located directly above the tunnel, that is, the odd-numbered pipe joint arrangement in the centrifugal test, the tunnel excavation notably causes the pipe to have a single sudden change in the joint position, and the settlement value is often higher than that of the continuous pipeline.

**3.2. Comparison with the Winkler and Pasternak Solutions under Different Geotechnical Conditions.** The Winkler and Pasternak models are widely used in theoretically predicting the deformation of pipelines affected by tunneling. A number of studies have shown that the calculation results of the Pasternak model considering the continuity of the foundation and the shear stiffness of the soil are more accurate than those of the Winkler model.

The equilibrium differential equation for the load on the pipeline on the Winkler subgrade is

$$E_p I_p \frac{d^4 w_p(x)}{dx^4} + \text{KD} w_p(x) = q(x)D. \quad (19)$$

The equilibrium differential equation for the load on the pipeline on the Pasternak subgrade is

$$\frac{d^4 w(x)}{dx^4} - \frac{\text{GD}}{E_p I_p} \frac{d^2 w(x)}{dx^2} + \frac{\text{KD}}{E_p I_p} w(x) = \frac{q(x)D}{E_p I_p}. \quad (20)$$

We first solve equations (19) and (20) under a concentrated load and then integrate them to obtain the pipeline settlement caused by tunneling.

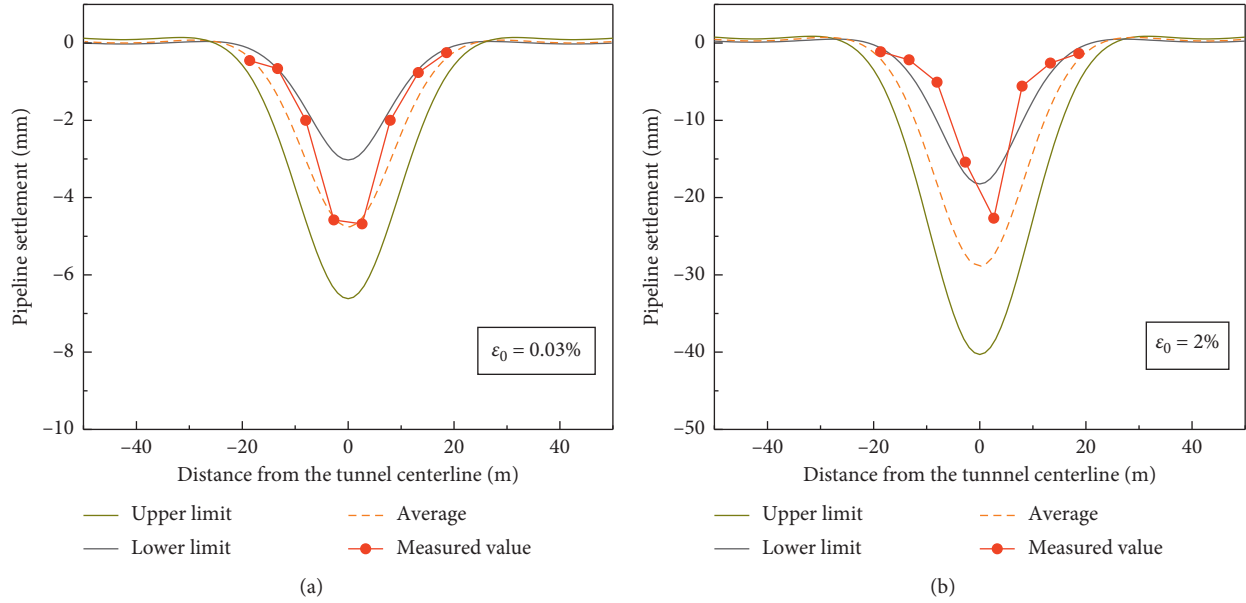
In order to verify the rationality of the energy solution and its applicability under different geotechnical conditions, based on the test and site conditions, four calculation parameters under different geotechnical conditions were selected, including sand layer [7], medium clay [29], very hard clay [30], and gravel formation [31]. The prediction results of the Winkler and Pasternak models are compared with the energy solutions proposed in this study under different geotechnical conditions, as shown in Figure 4. The calculation parameters are shown in Tables 1 and 2, respectively.

It can be seen from the comparison results in Figure 4 that the maximum settlement value of the pipeline



TABLE 1: Calculation parameters of pipeline and soil.

Tunnel radius (m)	Pipeline depth (m)	Tunnel depth (m)	Pipeline diameter (m)	Pipeline bending stiffness ( $\text{kN}\cdot\text{m}^2$ )	Soil elastic modulus (MPa)	Poisson's ratio
2.25	4.165	11.25	1.19	$3.36 \times 10^6$	19.52	0.3

FIGURE 3: Comparison of the energy solution in this study with the centrifugal test: (a) volume losses  $\epsilon_0 = 0.03\%$ ; (b) volume losses  $\epsilon_0 = 2\%$ .

calculated by the Pasternak model considering the influence of soil shear stiffness is larger than the Winkler model. This phenomenon is relatively obvious in the clay layer. In the sand layer, the displacement mode of the soil approximates the limit state 1 ( $d \approx 0$ ), and the calculation results of the Winkler and Pasternak models are very close to the lower limit curve solved by the energy solution, which is consistent with the expected results. By comparing the calculation results under four different geotechnical conditions, it can be seen that, as the soil changes from sand to clay, the displacement mode of the soil changes, the focus gradually moves downward, and the calculation curves of the Winkler and Pasternak models also gradually deviate from the lower limit value and move closer to the average value curve. When the geotechnical condition changes from medium clay to very hard clay or gravel formation, the calculation curves of the Winkler and Pasternak models further deviate from the average value and approach the upper limit curve. By comparing the results of the centrifugal test with the existing theoretical calculation results, the energy solution proposed in this study, considering the uniform ground movement model of soil, can be used to predict the pipeline settlement caused by tunneling. Furthermore, for the displacement of the pipeline under different geotechnical conditions, the settlement interval calculated in this study can well envelop the prediction curves of the Winkler and Pasternak models.

#### 4. Engineering Application

Based on the case of tunneling under the rainwater pipe culvert in a section of Hefei Metro Line 4 in China, the analysis method proposed in this study is used to predict the pipeline response caused by tunnel excavation. The curved tunnel with radius of curvature  $r = 350$  m is constructed using the shield method. During construction, the tunnel vertically passes through a deep buried concrete rainwater pipeline with a diameter of  $D = 1.8$  m and a wall thickness of  $t = 0.18$  m. This relationship is shown in Figure 5. In the construction of the double line tunnel, the left and right shields are used in turn, and the distance between two lines is about 20 m. This study discusses only the pipeline response caused by the left-line shield construction. The relevant parameters of the pipeline and soil are shown in Table 3. During construction, the monitoring points are arranged on the upper surface of the pipeline by means of drilling, which is used to monitor the pipeline settlement caused by tunneling in real time. The position and spacing of the monitoring points are shown in Figure 5(b).

As the excavation and grouting in the shield process will affect the pipeline settlement, a three-dimensional finite element model is established to simulate the shield construction process. In order to facilitate the comparison with the calculation results of the energy method, the construction process of the left-line tunnel is also used for simulation analysis. Figure 6 shows the finite element model

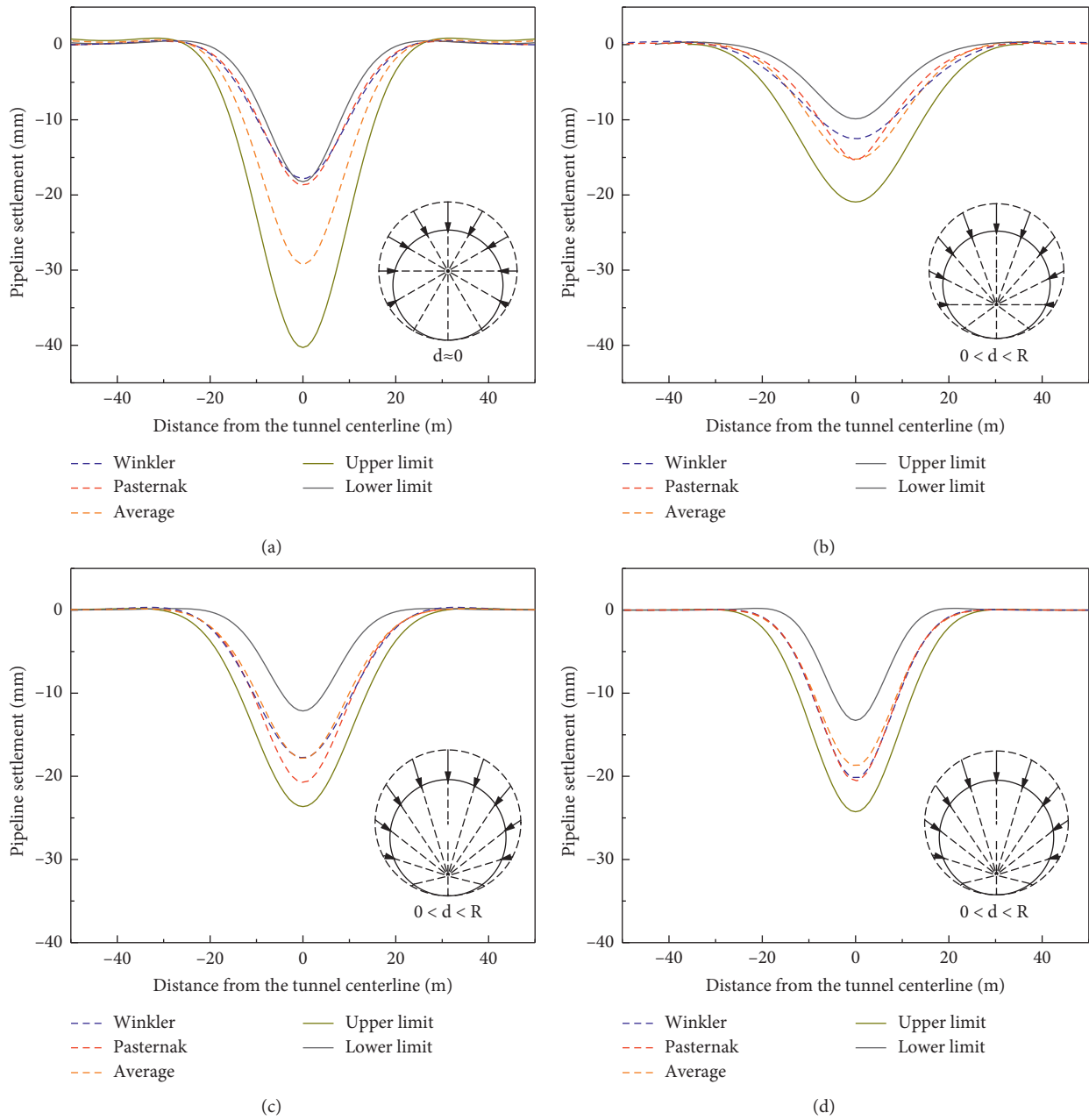


FIGURE 4: Comparison of the energy solutions calculated in this study with the Winkler and Pasternak solutions: (a) sand layer; (b) medium clay; (c) very hard clay; and (d) gravel formation.

TABLE 2: Calculation parameters of pipeline and soil.

Geotechnical conditions	Tunnel radius (m)	Pipeline depth (m)	Tunnel depth (m)	Pipeline diameter (m)	Pipeline bending stiffness ( $\text{kN}\cdot\text{m}^2$ )	Soil elastic modulus (MPa)	Poisson's ratio
Medium clay	3	12.3	15	3	$5.63 \times 10^6$	8.2	0.3
Very hard clay	3	6	15	2	$5.63 \times 10^6$	41.5	0.21
Gravel	3	5.5	14	0.8	$8.25 \times 10^5$	37.8	0.29

of tunneling under the rainwater pipe culvert. The overall model contains approximately 75,000 nodes and 120,000 elements. The soil and underground pipelines are simulated by solid elements, and the outer casing of the shield machine

and lining are simulated by the plate elements. The segmentation of the shield and the segmental installation of the lining are considered in the model, ignoring the influence of the longitudinal section of the concrete segment.

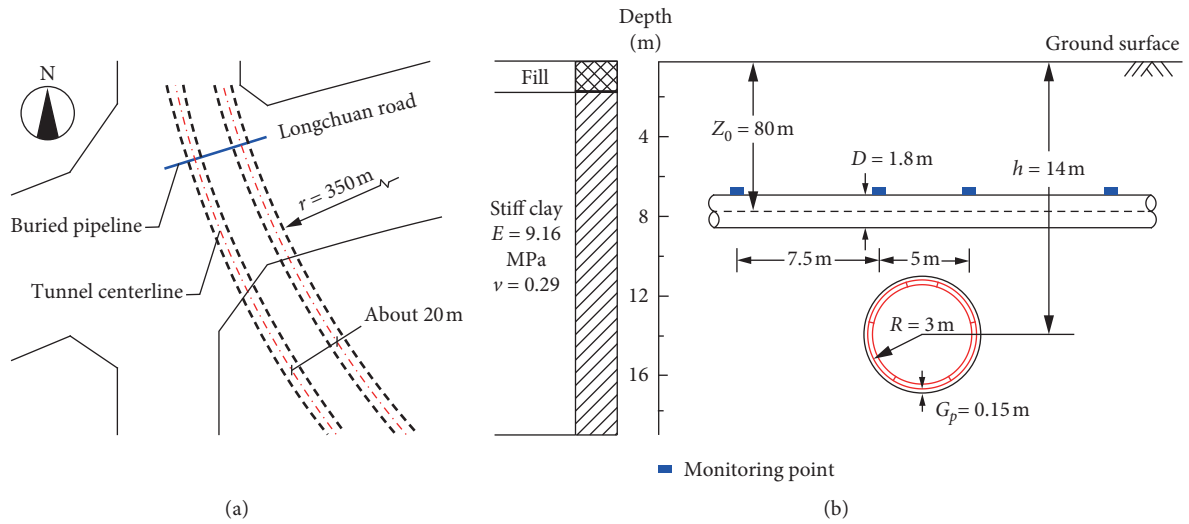


FIGURE 5: The cross-over relationship between the tunnel and pipeline and the placement of measuring points: (a) plan view; (b) section view and points arrangement.

TABLE 3: Parameters of pipeline and soil.

Tunnel radius (m)	Pipeline depth (m)	Tunnel depth (m)	Pipeline diameter (m)	Pipeline bending stiffness ( $\text{kN}\cdot\text{m}^2$ )	Soil elastic modulus (MPa)	Poisson's ratio	Volume losses
3	8	14	1.8	$1.82 \times 10^7$	9.16	0.29	0.0184

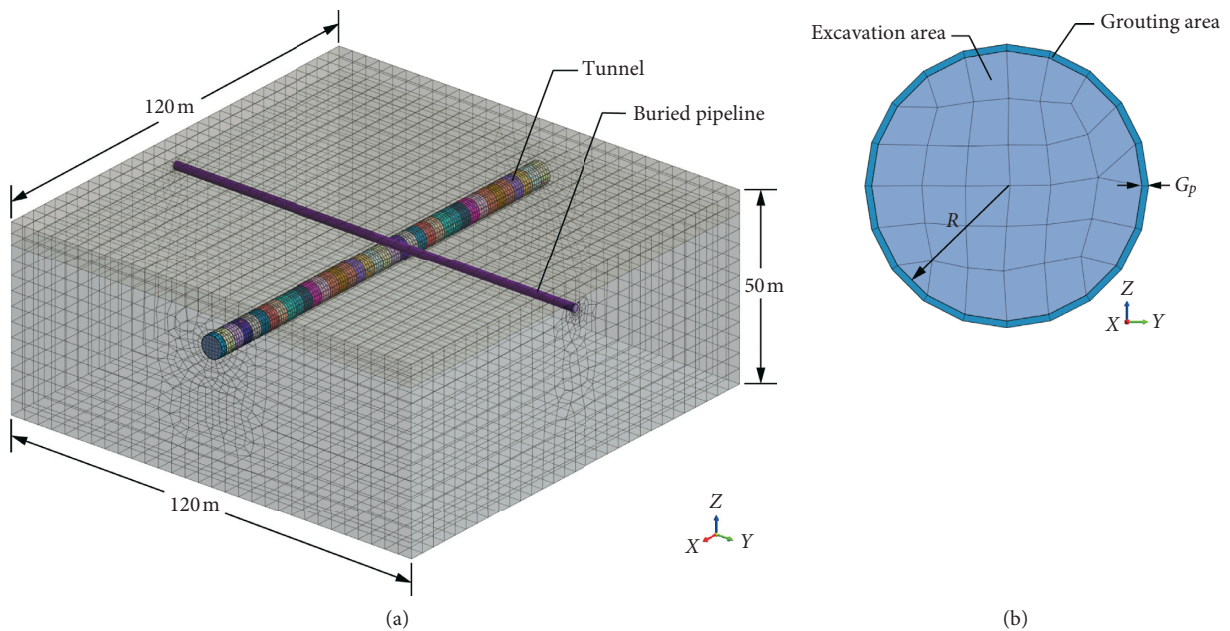


FIGURE 6: Three-dimensional finite element model: (a) 3D view; (b) tunnel profile.

Synchronous grouting during tunnel construction is simulated by changing the element properties of the reserved grouting area.

Figure 7 shows a comparison of the energy solutions, simulation results, and field measurements. The measured values are well enveloped in the settlement interval

calculated theoretically in this study and are also closer to the average curve. Compared to the average calculated by the energy method, the measured settlement trough width is slightly smaller. Therefore, for clay to hard clay soil conditions, the upper limit is used in the design stage to predict the settlement of the pipeline with certain redundancy safety.



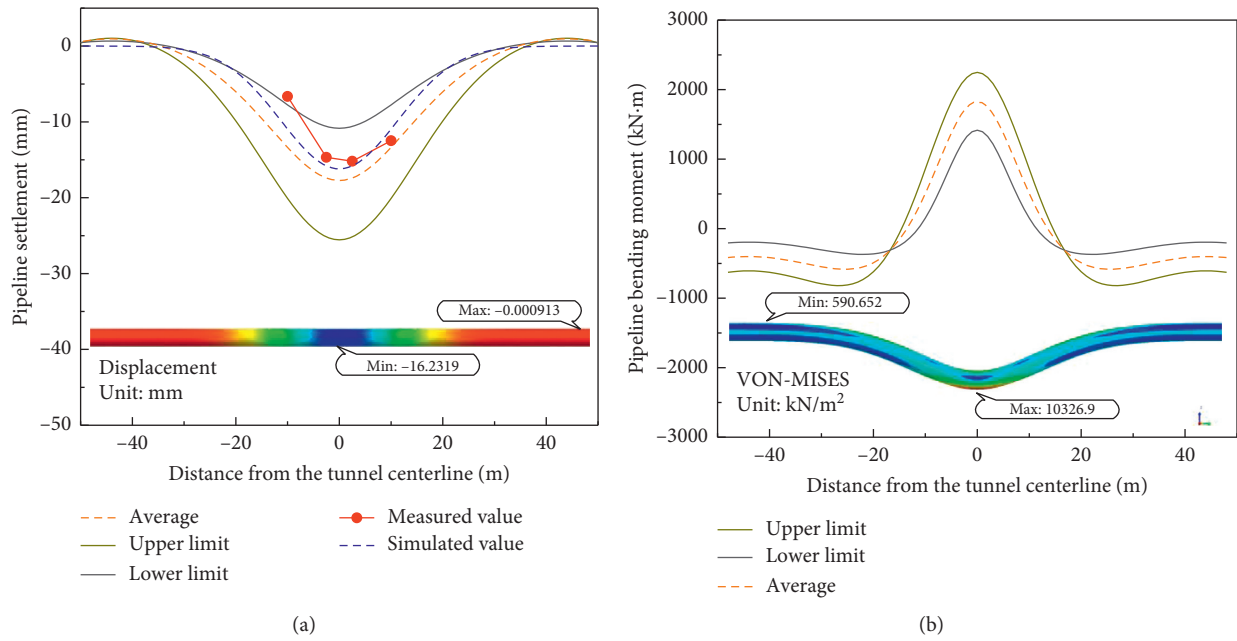


FIGURE 7: Calculation results and measured values of the pipeline response caused by the tunnel: (a) pipeline settlement; (b) pipeline bending moment.

In the construction stage, the average value should be used to predict the settlement of the pipeline more accurately and reliably.

Figure 7(b) shows the longitudinal bending moment distribution curve calculated by the energy solution and includes the MISES stress distribution of the pipeline calculated by the finite element method. The results show that the positive bending moment of the tunnel at the center point of the pipeline ( $x=0$  m) is the largest. In the hard clay stratum of this site, the average curve is used as the pipeline deformation prediction curve, and the maximum bending moment reaches 1.832 MN m. This result indicates that the bottom of the section pipeline is in the most unfavorable state of tension. At  $x=13.5$  m, the pipeline bending moment is 0, indicating that the section has the highest shear value. At  $x=25$  m, the negative bending moment value of the pipeline is the largest ( $-0.585$  MN m), indicating that the top section of the pipeline is in the most unfavorable state of tension. The monitoring and protection of the abovementioned three most unfavorable pipeline sections should be strengthened during construction to minimize adverse impacts.

The shield section of the project is a tunnel with a small radius of curvature. Compared with the linear tunnel, the construction difficulty is greatly increased, and the requirements for the engineers are higher. In actual construction, there are staggered deformations of the segment at the longitudinal and transverse joints, as well as leakage at the seam locations, as shown in Figure 8. In the tunnel construction, there are segment dislocations at the longitudinal and transverse joints, as well as leakage at the seam location, as shown in Figure 8. There is a difference between changing the element properties of the grouting area in the numerical simulation and the timeliness of synchronized

grouting and secondary grouting in actual construction. These factors make the numerical simulation results no longer applicable under working conditions where the construction factors exert great influence, and a method that takes into account the prediction accuracy and the redundancy safety method needs to be applied.

According to the foregoing analysis, the steps of predicting the pipeline response using the energy solution based on the uniform ground movement model proposed in this study can be summarized as follows:

- (1) Determine the calculation parameters, including the outer radius of the tunnel  $R$ , the geometric gap  $G_p$  between the shield machine and the lining, the peak value  $S_{max}$ , and the width coefficient  $i$  of the settlement trough. Then, the free displacement field of soil around the pipeline due to tunneling is calculated based on the uniform ground movement model. In the actual project, in order to make the calculation results of the energy solution more accurate, the free displacement field of the soil can be obtained by fitting the measurements using the Peck formula.
- (2) The total potential energy equation is obtained by superimposing the pipeline bending strain energy  $U$  and the earth pressure on the pipeline work  $W$ . Then, the variation of the total potential energy equation is used to obtain the governing equation. The free displacement field is brought into the governing equation to determine the appropriate calculation accuracy. Generally, the 10th-order Fourier series is used to calculate the pipeline settlement prediction interval caused by the shield, including the upper and lower limits and the average value. After determining the appropriate calculation accuracy, the

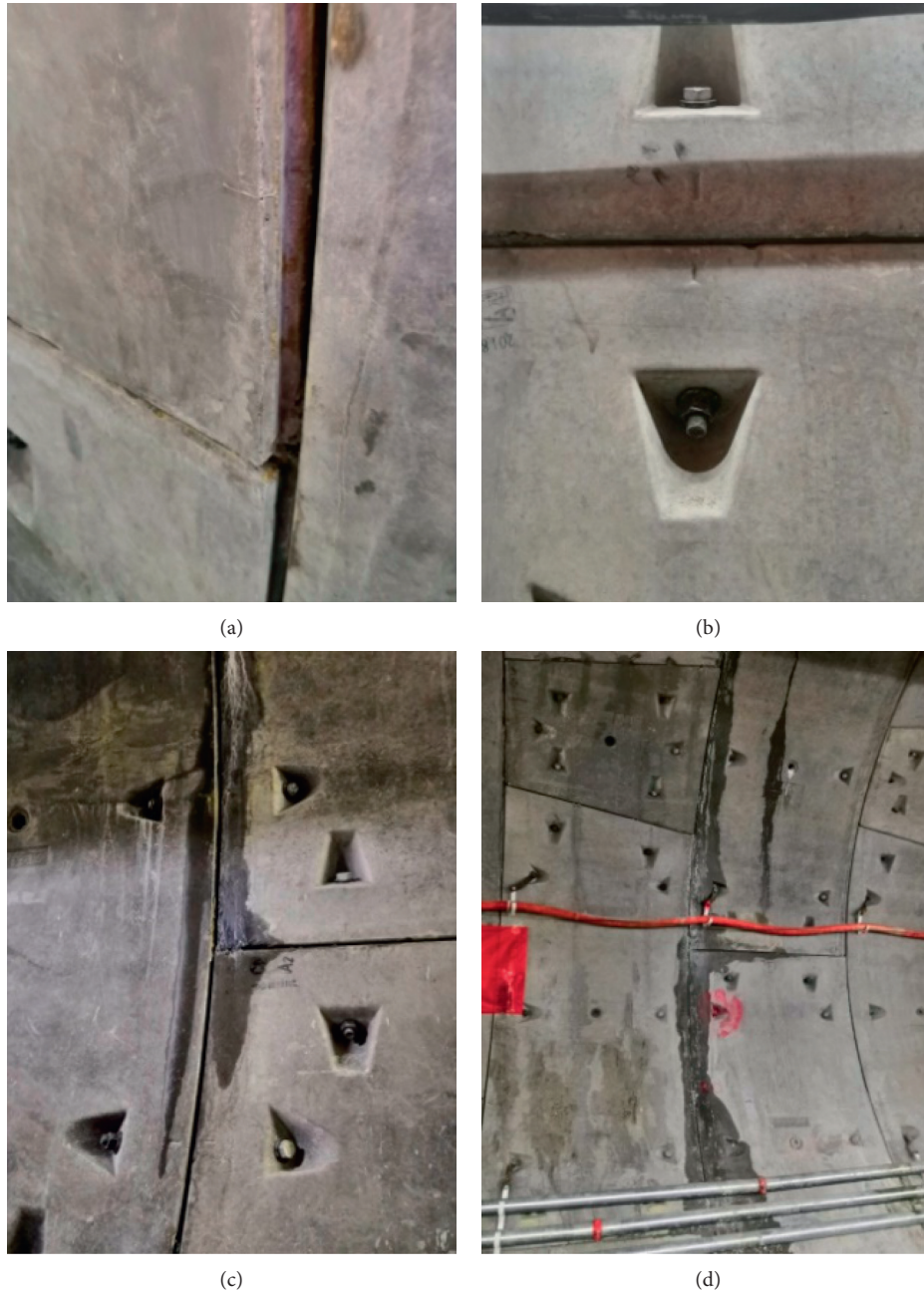


FIGURE 8: Adverse effects of construction factors: (a) transverse dislocation; (b) longitudinal dislocation; (c) leakage; (d) secondary grouting.

10th-order Fourier series is generally taken, and the free-displacement field is brought into the governing equation to calculate the pipeline settlement prediction interval induced by tunneling, including the upper and lower limits and the average value.

- (3) According to the geotechnical conditions of the site, select the appropriate pipeline response prediction curve. For the site conditions of sand and soft soil, we recommend selecting the average of the theoretical calculations in the design stage to ensure redundant safety. In the construction stage, the lower limit is selected to predict the pipeline settlement. For

medium clay, hard clay, and gravel formation, the upper limit and average should be chosen separately during the design and construction phases. Finally, according to the selected calculation curve, the most unfavorable position profile of the pipeline caused by tunnel excavation is determined, and key monitoring or protection measures are taken during construction.

## 5. Conclusions

Based on the uniform ground movement model, this study proposes an energy analysis method for predicting pipeline

settlement caused by tunneling. The following conclusions are drawn.

- (1) The applicability of the energy solution is verified by comparing the pipeline settlement interval calculated by this method with the centrifugal test and the Winkler and Pasternak solution. In addition, for the settlement of pipelines caused by tunneling under different geotechnical conditions, the settlement interval calculated by energy solution can well envelop the theoretical prediction curves calculated by the Winkler and Pasternak model.
- (2) Combined with engineering examples, the energy solution is used to predict pipeline settlement and bending moment distribution. The theoretically calculated settlement interval can accurately cover the measured values and, at the same time, predict the most unfavorable section of the pipeline to determine the key monitoring and protection objects in the construction process. Although the numerical simulation can calculate a specific value, it cannot consider the quality of the shield construction and the timeliness of synchronized grouting and secondary grouting in actual construction. The results are often different from the measured values.
- (3) The calculation method proposed in this study can consider the influence of different geotechnical conditions on pipeline deformation. For the site conditions of sand and soft soil, it is recommended to select the average value of the theoretical calculation in the design stage to ensure redundant safety. The lower limit value is selected as the prediction curve of pipeline settlement in the construction stage. For medium clay, hard clay, and gravel formation, the upper limit and average should be chosen separately during the design and construction phases.

## Data Availability

The data used to support the findings of this study are available from the corresponding author upon request.

## Conflicts of Interest

The authors declare that there are no conflicts of interest regarding the publication of this paper.

## Acknowledgments

This work was supported by the National Natural Science Foundation of China (grant no. 51878005).

## References

- [1] M. Huang, X. Zhou, J. Yu, C. F. Leung, and J. Q. W. Tan, "Estimating the effects of tunnelling on existing jointed pipelines based on Winkler model effects of tunnelling on existing jointed pipelines based on Winkler model," *Tunnelling and Underground Space Technology*, vol. 86, pp. 89–99, 2019.
- [2] J. Yu, C. Zhang, and M. Huang, "Soil-pipe interaction due to tunnelling: assessment of winkler modulus for underground pipelines," *Computers and Geotechnics*, vol. 50, pp. 17–28, 2013.
- [3] P. Ni and S. Mangalathu, "Fragility analysis of gray iron pipelines subjected to tunneling induced ground settlement," *Tunnelling and Underground Space Technology*, vol. 76, pp. 133–144, 2018.
- [4] X. Q. Liu, F. Y. Liang, H. Zhang et al., "Energy variational solution for settlement of buried pipeline induced by tunneling," *Rock Soil Mechanics*, vol. 35, pp. 217–223, 2014, in Chinese.
- [5] M. S. Saiyar, W. A. Take, and I. D. Moore, "Post-failure fracture angle of brittle pipes subjected to differential ground movements," *Tunnelling and Underground Space Technology*, vol. 49, pp. 114–120, 2015.
- [6] S. Ma, Y. Liu, X. Lv, Y. Shao, and Y. Feng, "Settlement and load transfer mechanism of pipeline due to twin stacked tunneling with different construction sequences," *KSCE Journal of Civil Engineering*, vol. 22, no. 10, pp. 3810–3817, 2018.
- [7] T. E. Vorster, A. Klar, K. Soga, and R. J. Mair, "Estimating the effects of tunneling on existing pipelines," *Journal of Geotechnical and Geoenvironmental Engineering*, vol. 131, no. 11, pp. 1399–1410, 2005.
- [8] K. Y. Zhang, J. L. C. Torres, and Z. J. Zang, "Numerical analysis of pipelines settlement induced by tunneling," *Advances in Civil Engineering*, vol. 2019, Article ID 4761904, 10 pages, 2019.
- [9] G. Cocchetti, C. di Prisco, A. Galli, and R. Nova, "Soil-pipeline interaction along unstable slopes: a coupled three-dimensional approach. Part I: theoretical formulation," *Canadian Geotechnical Journal*, vol. 46, no. 11, pp. 1289–1304, 2009.
- [10] J. Zhang, R. Xie, and H. Zhang, "Mechanical response analysis of the buried pipeline due to adjacent foundation pit excavation," *Tunnelling and Underground Space Technology*, vol. 78, pp. 135–145, 2018.
- [11] J. Shi, X. Zhang, L. Chen, and L. Chen, "Numerical investigation of pipeline responses to tunneling-induced ground settlements in clay," *Soil Mechanics and Foundation Engineering*, vol. 54, no. 5, pp. 303–309, 2017.
- [12] Y. Wang, J. Shi, and C. W. W. Ng, "Numerical modeling of tunneling effect on buried pipelines," *Canadian Geotechnical Journal*, vol. 48, no. 7, pp. 1125–1137, 2011.
- [13] G. Wei, "Establishment of uniform ground movement model for shield tunnels," *Chinese Journal of Geotechnical Engineering*, vol. 4, pp. 554–559, 2007, in Chinese.
- [14] J. H. L. Palmer and D. J. Belshaw, "Deformations and pore pressures in the vicinity of a precast, segmented, concrete-lined tunnel in clay," *Canadian Geotechnical Journal*, vol. 17, no. 2, pp. 174–184, 1980.
- [15] K. H. Park, "Elastic solution for tunneling-induced ground movements in clays," *International Journal of Geomechanics*, vol. 4, no. 4, pp. 310–318, 2004.
- [16] N. Loganathan and H. G. Poulos, "Analytical prediction for tunneling-induced ground movements in clays," *Journal of Geotechnical and Geoenvironmental Engineering*, vol. 124, no. 9, pp. 846–856, 1998.
- [17] C. Sagaseta, "Analysis of undrained soil deformation due to ground loss," *Géotechnique*, vol. 37, no. 3, pp. 301–320, 1987.
- [18] K. M. Lee, R. K. Rowe, and K. Y. Lo, "Subsidence owing to tunnelling. I. Estimating the gap parameter," *Canadian Geotechnical Journal*, vol. 29, no. 6, pp. 929–940, 1992.
- [19] A. Klar and A. M. Marshall, "Linear elastic tunnel pipeline interaction: the existence and consequence of volume loss equality," *Géotechnique*, vol. 65, no. 9, pp. 788–792, 2015.

- [20] S. Ma, Y. Shao, Y. Liu, J. Jiang, and X. Fan, "Responses of pipeline to side-by-side twin tunnelling at different depths: 3D centrifuge tests and numerical modelling," *Tunnelling and Underground Space Technology*, vol. 66, pp. 157–173, 2017.
- [21] A. Klar, A. M. Marshall, K. Soga, and R. J. Mair, "Tunneling effects on jointed pipelines," *Canadian Geotechnical Journal*, vol. 45, no. 1, pp. 131–139, 2008.
- [22] J. Shi, Y. Wang, and C. W. W. Ng, "Numerical parametric study of tunneling-induced joint rotation angle in jointed pipelines," *Canadian Geotechnical Journal*, vol. 53, no. 12, pp. 2058–2071, 2016.
- [23] B. P. Wham, C. Argyrou, and T. D. O'Rourke, "Jointed pipeline response to tunneling-induced ground deformation," *Canadian Geotechnical Journal*, vol. 53, no. 11, pp. 1794–1806, 2016.
- [24] J. Shi, W. Yu, and C. W. W. Ng, "Three-dimensional centrifuge modeling of ground and pipeline response to tunnel excavation," *Journal of Geotechnical and Geoenvironmental Engineering*, vol. 142, no. 11, 2016.
- [25] A. Klar, T. E. Vorster, K. Soga, R. J. Mair et al., "Elastoplastic solution for soil-pipe-tunnel interaction," *Journal of Geotechnical and Geoenvironmental Engineering*, vol. 133, no. 7, pp. 782–792, 2007.
- [26] R. J. Mair, R. N. Taylor, and A. Bracegirdle, "Subsurface settlement profiles above tunnels in clays," *Géotechnique*, vol. 43, no. 2, pp. 315–320, 1993.
- [27] A. D. Kerr, "On the determination of foundation model parameters," *Journal of Geotechnical Engineering*, vol. 111, no. 11, pp. 1334–1340, 1985.
- [28] L. Xu, Research on longitudinal settlement of shield tunnel in soft ground, Ph.D. Thesis, Tongji University, Shanghai, China, 2005, in Chinese.
- [29] W. Y. Wu, Y. K. Sun, and T. Q. Zhang, "Analysis of the effects on the adjacent underground pipelines by shield tunneling construction," *China Railway Science*, vol. 29, pp. 58–62, 2008, in Chinese.
- [30] W. Y. Wu, Study on mechanical behaviors of buried pipelines induced by shield tunneling construction, Ph.D. Thesis, Zhejiang University, Hangzhou, China, 2008, in Chinese.
- [31] K. L. Zheng, Study on influence law of shield construction on underground pipeline in fu-nan section of nanning subway, Xi'an University of Science and Technology, Xi'an, China, 2019, in Chinese.